The [URE3] Yeast Prion Results from Protein Aggregates That Differ from Amyloid Filaments Formed in Vitro

Leslie Ripaud, Laurent A Maillet, Fabien Durand, Françoise Immel-Torterotot, Christophe Cullin

THE JOURNAL OF BIOLOGICAL CHEMISTRY
Vol. 279, No. 49, Issue of December 3, pp. 50962–50968, 2004
Printed in U.S.A.

The [URE3] Yeast Prion Results from Protein Aggregates That Differ from Amyloid Filaments Formed *in Vitro**

Received for publication, August 2, 2004, and in revised form, September 16, 2004
Published, JBC Papers in Press, September 28, 2004, DOI 10.1074/jbc.M408792200

Leslie Ripaud‡, Laurent Maillet, Françoise Immel-Torterotot, Fabien Durand, and Christophe Cullin§

From the Institut de Biochimie et Génétique Cellulaires, 1, rue Camille Saint Saëns, UMR 5095, CNRSI Université Bordeaux 2 Victor Segalen, 33077 Bordeaux cedex France

The [URE3] yeast prion is a self-propagating inactive form of the Ure2 protein. Ure2p is composed of two domains, residues 1–93, the prion-forming domain, and the remaining C-terminal part of the protein, which forms the functional domain involved in nitrogen catabolite repression. *In vitro*, Ure2p forms amyloid filaments that have been proposed to be the aggregated prion form found *in vivo*. Here we showed that the biochemical characteristics of these two species differ. Protease digestions of Ure2p filaments and soluble Ure2p are comparable when analyzed by Coomassie staining as by Western blot. However, this finding does not explain the pattern specifically observed in [URE3] strains. Antibodies raised against the C-terminal part of Ure2p revealed the existence of proteolysis sites efficiently cleaved when [URE3], but not wild-type crude extracts, were submitted to limited proteolysis. The same antibodies lead to an equivalent digestion pattern when recombinant Ure2p (either soluble or amyloid) was analyzed in the same way. These results strongly suggest that aggregated Ure2p in [URE3] yeast cells is different from the amyloid filaments generated *in vitro*.

Prion proteins are misfolded proteins that propagate through their interaction with the normal (correctly folded) host protein. The prion concept, initially launched in 1967 (1) and clearly established in 1982 (2), is the result of several decades of studies related to mammalian transmissible spongiform encephalopathies. The prion protein involved in this pathological process is PrP. The cellular isoform PrP^{c} consists mainly of α-helices, whereas its pathological isoform PrP^{Sc} represents predominantly β-sheets (3). PrP^{Sc} is prone to aggregation and is protease-resistant. Only very recently, protease-resistant PrP aggregates generated *in vitro* have been reported to be infectious (4). However, the exact nature of the infectious agent remains unknown.

The yeast *Saccharomyces cerevisiae* contains several proteins with prion-like properties (5–7). Because the "prionization" mechanism has been conserved through evolution (8), they are highly tractable models for studying the mechanisms of prion propagation. The most extensively studied yeast prion proteins are Ure2p and Sup35p, responsible for the [URE3] and [PSI] phenotypes, respectively. Ure2p is a regulator of nitrogen catabolite repression (NCR)[1] sensitive transcription in *S. cerevisiae* (9, 10). In the presence of a good nitrogen source (asparagine, ammonia, or glutamine) Ure2p complexes with the Gln3p transcription factor in the cytoplasm (11, 12), thus preventing the transcription of genes expressed upon nitrogen starvation. One of these genes is *DAL5*, which encodes a permease for ureidosuccinate (Usa) (13). As the prion isoform of Ure2p is inactive, *DAL5* is expressed in [URE3] cells, and the yeast are capable of importing Usa thus permitting the growth in selective medium (14). Sup35p is a component of the translation termination factor in *S. cerevisiae* (15). [PSI] prion causes partial read through of stop codons (16). These two proteins have an asparagine/glutamine-rich N-terminal domain, called the prion-forming domain (PFD), which is necessary and sufficient to propagate the prion state.

The nature of the conformational changes between the cellular and the prion isoforms of these proteins was largely investigated but still remains unclear. The self-propagating species especially, called propagon, has not been yet characterized. A clear link exists between the yeast prion phenotype and the aggregation of the protein involved in this process. The [PSI] model is the most documented. In [PSI] yeast cells, Sup35p aggregates and is found in the pellet fraction in sedimentation assays (17, 18). The Sup35-green fluorescent protein fusion proteins form several foci in yeast cells that bear [PSI] (18). Moreover, Sup35p forms amyloid fibrils *in vitro* (19), which are infectious and recapitulate all strain properties when introduced in yeast cells (20, 21).

Like Sup35p, Ure2p has similar properties of assembly into amyloid fibrils *in vitro* (22). In a test tube, the N-terminal PFD connects each subunit and forms an amyloid filament backbone surrounded by the C-terminal moieties (23). However, the role of aggregation in [URE3] prion propagation is controversial. Ure2-green fluorescent protein fusion proteins only form foci in [URE3] yeast cells (24) under experimental conditions leading to the elimination of the prion (25–27). Otherwise the fluorescence remains diffuse. Sedimentation assays also led to contradictory results. Although Schlumpberger *et al.* (28) observed increased aggregation in [URE3] cells, the only difference we noticed is a decrease in Ure2p concentration measured in a Western blot of a crude extract of the [URE3] strains(27).

In this work we have investigated these discrepancies. We observed that Ure2p is actually aggregated in [URE3] cells. These aggregates behave differently from the Sup35p aggregates found in [PSI]-containing cells. The Ure2p aggregates are resistant to boiling in 2% SDS buffer and need strong denaturing agents to be detected on Western blots. We determined the

* The costs of publication of this article were defrayed in part by the payment of page charges. This article must therefore be hereby marked "*advertisement*" in accordance with 18 U.S.C. Section 1734 solely to indicate this fact.
‡ Supported by a BDI "CNRS-Région Aquitaine" fellowship.
§ To whom correspondence should be addressed. Tel.: 33-556-999-017; Fax: 33-556-999-017; E-mail: Christophe.Cullin@ibgc.u-bordeaux2.fr.

[1] The abbreviations used are: NCR, nitrogen catabolite repression; Usa, ureidosuccinate; PFD, prion-forming domain.

amount of Ure2p required to give a wild-type phenotype and concluded that in [URE3] yeast cells, the aggregated protein should be inactive. We further characterized [URE3] aggregates by limited proteolysis using antibodies raised against the full-length protein. We could definitively confirm that Ure2p is not proteolyzed in the same way in [URE3] or in wild-type yeast cells. Next, we used antibodies raised against the C-terminal part of Ure2p to analyze the proteolyzed species. As the proteolysis pattern of Ure2p in [URE3] is not consistent with the amyloid pattern of Ure2p (23, 29), we produced both soluble and amyloid Ure2p and compared their proteolysis pattern under the same experimental conditions. We concluded that the process in [URE3] leading to Ure2p aggregates differs from the process leading to amyloid fibers formed in a test tube.

EXPERIMENTAL PROCEDURES

Yeast Strains, Media, and Plasmids—The following strains of *S. cerevisiae* were used in this study. CC30 genotype is *trp1-1, ade2-1, leu2-3,112, his3-11,15,* Δ*ura2*::*HIS3*. The CC34 [URE3] strain is isogenic to CC30. The CC32 genotype is *trp1-1, ade2-1, leu2-3,112, his3-11,15,* Δ*ura2*::*HIS3, cyh2r,* Δ*ure2*::*CYH2*. Yeast transformations were carried out as described previously (30). Unless specified, yeasts were grown in YPD (1% bactoyeast extract, 1% bactopeptone, 2% dextrose, 20 mg/liter adenine). SD medium (0.67% yeast nitrogen base, 2% dextrose) was supplemented with 20 mg/liter adenine, 20 mg/liter tryptophan, and 60 mg/liter leucine. Either 20 mg/liter uracil or 15 mg/liter ureidosuccinate was added as specified in the text.

The pYe2L-URE2 BamHI-HpaI fragment containing the *URE2* open reading frame was cloned under the control of the *TET*-repressible promoter into pCM183 linearized with the same enzymes resulting in pCM183/URE2. *URE2* open reading frame was PCR-amplified from pUHE-URE2 and cloned into pET3a resulting in pET3a-URE2. The His_6 tag was PCR-amplified and inserted at the 3′-end of *URE2* resulting in pET3a-URE2tagHIS.

Antibodies Production and Purification—The AGTTPMSQSRFFDYP peptide corresponding to the Ure2p sequence from amino acids 284 to 298 was synthesized with an additional cysteine at the N terminus end coupled to hemocyanin. Rabbit antiserum was affinity-purified, and the specificity of this antibody was checked. No signal was detected in cells expressing a Ure2 protein truncated from the C-terminal domain (data not shown).

Protein Extraction, Sedimentation Analysis, and Western Blotting—Total yeast protein extracts were prepared by glass bead disruption in TNT buffer (25 mM Tris-Cl, pH 7.4, 100 mM NaCl, 0.2% Triton) containing 1 mM phenylmethylsulfonyl fluoride. Sedimentation analyses were performed as described previously (27). Samples were boiled for 5 min in 1× loading buffer (0.06 M Tris-Cl, pH 6.8, 2% SDS, 10% glycerol, 5% β-mercaptoethanol, 0.002% bromphenol blue). Urea was added to an 8 M final concentration in all samples unless otherwise specified. Proteins were separated by 12% SDS-PAGE. Gels were stained with Coomassie or used in Western blots to transfer proteins to a nitrocellulose membrane (Optitran BA-S83, Schleicher & Schuell). Membranes were probed with specific affinity-purified polyclonal antibodies raised against full-length Ure2p, against an Ure2p peptide corresponding to amino acids 284 to 298, and against Pap1p or Ade13p. Polyclonal peroxidase-conjugated anti-rabbit antibodies (Sigma) were used as secondary antibodies. Secondary antibody binding was detected with the SuperSignal reagent (Pierce) and the VersaDoc Imaging system (Bio-Rad). Signals were quantified with Quantity One software (Bio-Rad).

Limited Proteolysis—Protein extracts were prepared as described in TNT without protease inhibitors and clarified for 5 min at 1000 × *g*. 500 μg of yeast total protein extracts from CC30 and CC34 were diluted to 54 μl in TNT buffer, mixed with 6 μl of appropriate dilutions of proteinase K, and incubated at 37 °C for 30 min. Digestion was stopped by the addition of phenylmethylsulfonyl fluoride to a final concentration of 1 mM. Sample buffer and urea (to a final concentration of 8 M) were added, and samples were boiled for 5 min. Recombinant Ure2p was digested in the same way after a dilution of 60 μg of purified protein (soluble and amyloid fibrils) into 54 μl of TNT buffer. Alternatively 500 ng of amyloid fibrils were incubated in 500 μg of yeast total protein extracts from CC32 for 5 min before proteolysis.

Ure2p Expression, Purification, and Fibril Formation—Ure2p-His_6 was expressed from pET3a-URE2tagHIS in *Escherichia coli* BL21codon+DE3 strain (Stratagene) in LB medium containing 50 μg/ml ampicillin, 30 μg/ml chloramphenicol, and 50 μM isopropyl 1-thio-β-D-galactopyranoside. Induction was performed overnight at 18 °C. Cells were lysed by sonication in buffer A (50 mM sodium phosphate, 300 mM NaCl, pH 8). Insoluble material was removed by centrifugation for 15 min at 20,000 × *g*. Ure2p-His_6 was bound on nickel nitrilotriacetic acid-agarose (Qiagen), washed extensively with buffer A, and eluted with buffer B (50 mM sodium phosphate, 300 mM NaCl, 250 mM imidazole, pH 8). Imidazole was eliminated using a Sepharose G25 column (HiTrap desalting, Amersham Biosciences). The native conformation of soluble Ure2p was checked with circular dichroism spectroscopy (data not shown). Fibrils were assembled by incubating proteins at 1 mg/ml in buffer A at 4 °C during a 1–2 week period.

Electron Microscopy—Protein samples were loaded onto a 400 mesh copper electron microscopy grid coated with a plastic film (Formvar). To avoid rapid desiccation, sedimentation was allowed during a 10–30 min period in a moist Petri dish. Grids were then rinsed with 15–20 drops of freshly prepared 1% uranyl acetate in water (passed over 0.22-μm filter, Millipore), dried with filter paper, and observed with a Phillips Tecnai 12 Biowin electron microscope at 100 kV.

RESULTS

Urea Enhances Ure2p Detection from [URE3] Extracts in Western Blots—In a previous work, we found that the Ure2p signal intensity in Western blot experiments was very low in the [URE3] strain compared with the wild-type strain. This may be because of a lower Ure2p concentration in a prion-containing cell, or alternatively to a lower detection efficiency. The effect of denaturing agents like urea already used by others (28) was then tested. With our previous standard protocol we observed that the Ure2p signal intensity was 10 times lower in the CC34 [URE3] strain than in CC30 [ure3-0] (27). When urea was added to a final concentration of 8 M in the loading buffer, a 5-fold increase of this signal was observed (data not shown). This increase shows that most Ure2p [URE3] was not detected after boiling in 2% SDS buffer. To analyze whether the urea-sensitive fraction was soluble or aggregated, a 100,000 × *g* sedimentation assay was performed. Without urea, most Ure2p was detected in the supernatant fraction, whether the proteins were prepared from the wild-type or the [URE3] strains (Fig. 1*A*). Addition of urea after fractionation had no effect on the signal detected in wild-type extracts (Fig. 1*A*, *wt*, *columns S* and *P*). The intensity of the Ure2p species remained the same in both the pellet and the supernatant. In [URE3] extracts, the supernatant fraction exhibited the same intensity whether urea was added or not (Fig. 1*A*, *[URE3], column S*), whereas in the pellet fraction (Fig. 1*A*, *[URE3], column P*) the presence of urea strongly increased the detected signal. Thus, most Ure2p is aggregated in [URE3] cells. Without urea, this fraction (representing 80% of total Ure2p) is not efficiently detected on Western blot. In a previous work, Schlumpberger *et al.* (28) found that Ure2p was completely insoluble in [URE3] strains, whereas we found that even in [URE3] 20% remains soluble. The difference in the level of aggregation is in fact because of growth conditions. When CC34 [URE3] cells were grown overnight (for 5–7 generations) in rich medium YPD, 80% of the Ure2p signal was detected in the pellet fraction (Fig. 1, *B* and *C*). When the same strain was grown in SD + Usa (accordingly to the conditions used by Schlumpberger *et al.* (28)) no signal was detected in the supernatant (Fig. 1, *B* and *C*) indicating a complete aggregation of Ure2p. This result was also found for another yeast strain (Fig. 1*C*), indicating that this rather represents a general feature being independent of the genetic background of our strain. The SD + Usa medium is selective for the presence of [URE3] prion. However, decrease in Ure2p aggregation in non-selective medium could not be explained by a partial [URE3] curing in the population, because all the yeast cells remained [URE3] after growth in YPD (data not shown). As the SD + Usa medium is selective for the loss of function of Ure2p, enhanced aggregation of this protein in this medium might be because of a need

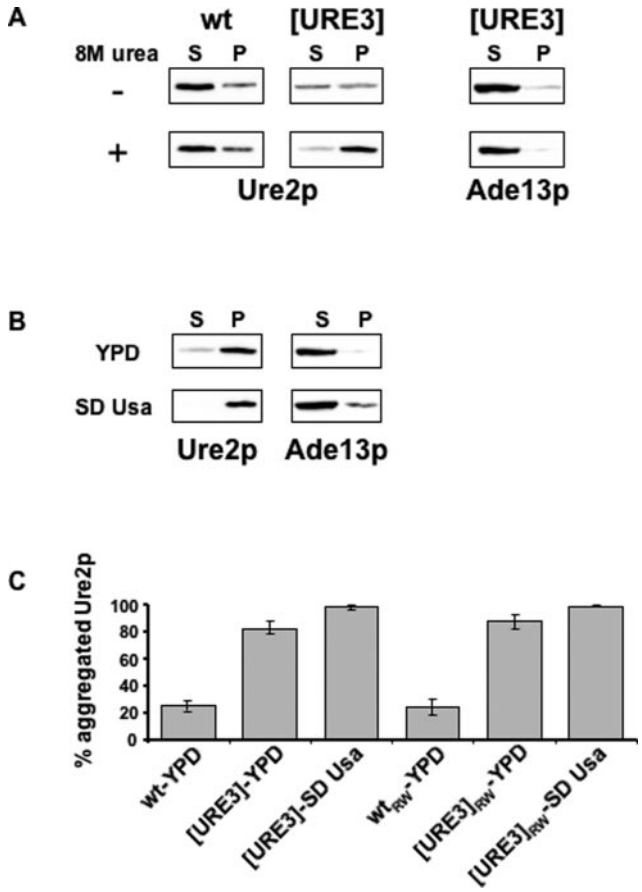

FIG. 1. **Analyses of Ure2p sedimentation in Western blots.** *A*, the effect of urea on the pellet fraction. The effect of 8 M urea was tested on protein extracts previously fractionated by an ultracentrifugation at 100,000 × *g* for 30 min. The extracts are attained from wild-type (*wt*) or [URE3] yeast cells. The Western blot was revealed with antibodies against Ure2p or Ade13p, a control protein. *S*, supernatant; *P*, pellet. *B*, influence of growth conditions on Ure2p solubility. After growing in SD + Usa, [URE3] cells were grown for 16 h either in YPD or SD + Usa. Total protein extracts were fractionated by an ultracentrifugation at 100,000 × *g* for 30 min. All samples were analyzed with 8 M urea. *C*, level of aggregation of Ure2p in different strains. The strain CC30 (*wt*), CC34 (*[URE3]*), 3686 (wt_{RW}) and YHE64 ($[URE3]_{RW}$) (24) were grown in SD + Usa medium and transferred for 16 h in YPD or SD + Usa medium as in *B*. The ratio of aggregated Ure2p was quantified using the Quantity One software. The mean represents three independent experiments.

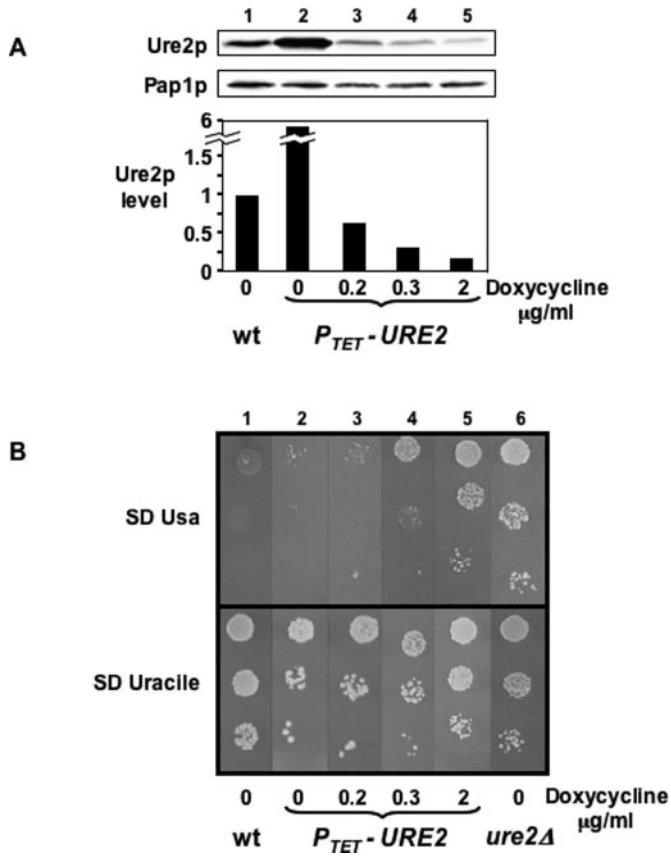

FIG. 2. **Estimation of Ure2p quantity sufficient to inhibit Usa uptake.** The *URE2* open reading frame was cloned under the control of the *TET*-repressible promoter in pCM183, creating pCM183/URE2. CC32 (*ure2*Δ) transformants with pCM183/URE2 are noted P_{TET}-*URE2*. In this strain Ure2p is under the control of the *TET*-repressible promoter. The CC30 (*wt*), CC32 (*ure2*Δ) and P_{TET}-*URE2* were grown overnight in liquid medium SD + uracil and doxycycline ranging from 0 to 2 µg/ml. *A*, then an aliquot of each culture was used to quantify Ure2p production by Western blot analysis. An antibody against Pap1p was used to normalize the quantification. The Ure2p level was finally expressed as a ratio based on the concentration found in the wild-type strain. *B*, another aliquot of liquid cultures was used to test for the complementation phenotype. Growth was compared on SD + Usa and SD + uracil, both containing the same concentration of doxycycline as each liquid culture tested. The absence of growth on SD + Usa indicates complementation.

of its complete inactivation. To test for this hypothesis, we investigated which amount of Ure2p was required for the wild-type phenotype (absence of growth in SD + Usa).

Ure2p Quantity Sufficient to Inhibit Usa Uptake—The *URE2* open reading frame was cloned upstream of a tetracycline-repressible promoter in the pCM183/URE2 plasmid. This plasmid was transformed into the CC32 *ure2*Δ. In this strain, *URE2* expression is inversely proportional to the doxycycline concentration in the medium. Without doxycycline, a 5-fold increase in Ure2p level was observed compared with wild-type cells (Fig. 2*A*, compare *columns 1* and *2*). The Ure2p level was quantified by comparing the signal obtained with antibodies against Ure2p, to the one obtained with antibodies to poly(A) Pap1p (31), a protein not involved in prion processes. Using 0.2 µg/ml of doxycycline, the level of Ure2p production was about 60% of the wild-type level (Fig. 2*A*, *column 3*). This is sufficient for the complementation of the *URE2* deletion in CC32. No growth was observed on SD + Usa, as for the controls without doxycycline in wild-type and P_{TET}-*URE2* strains (Fig. 2*B*, *columns 1–3*). One third of the wild-type Ure2p level, which was obtained with 0.3 µg/ml of doxycycline, leads to an incomplete complementation phenotype (Fig. 2, *A* and *B*, *column 4*). The growth on SD + Usa is heterogeneous. Using 2 µg/ml of doxycycline, the Ure2p level is about 15% of the wild-type level. In this condition, yeast cells clearly grow on SD + Usa as the *ure2*Δ control (Fig. 2*B*, *columns 5* and *6*). These results suggest that less than 15% of Ure2p (in comparison to the wild-type level) gives rise to a mutant phenotype. If aggregation leads to Ure2p inactivation, then a complete aggregation of Ure2p is not required to obtain the mutant [URE3] phenotype. We next investigated the biochemical nature of the aggregated form of Ure2p in [URE3] cells.

$Ure2p^c$- and $Ure2p^{[URE3]}$-limited Proteolysis—We further characterized these aggregates by limited proteolysis. This is a tool to investigate protein structure, as flexible regions are more sensitive to proteolysis than folded polypeptide chains. Moreover, the core of ordered aggregates has a lower accessibility to proteases and is expected to be very resistant to proteolysis. Proteins extracted from wild-type and [URE3] strains were digested for 30 min with proteinase K concentrations ranging from 0 to 15 µg/ml. As proteins were extracted and incubated without protease inhibitors for 30 min, each sample

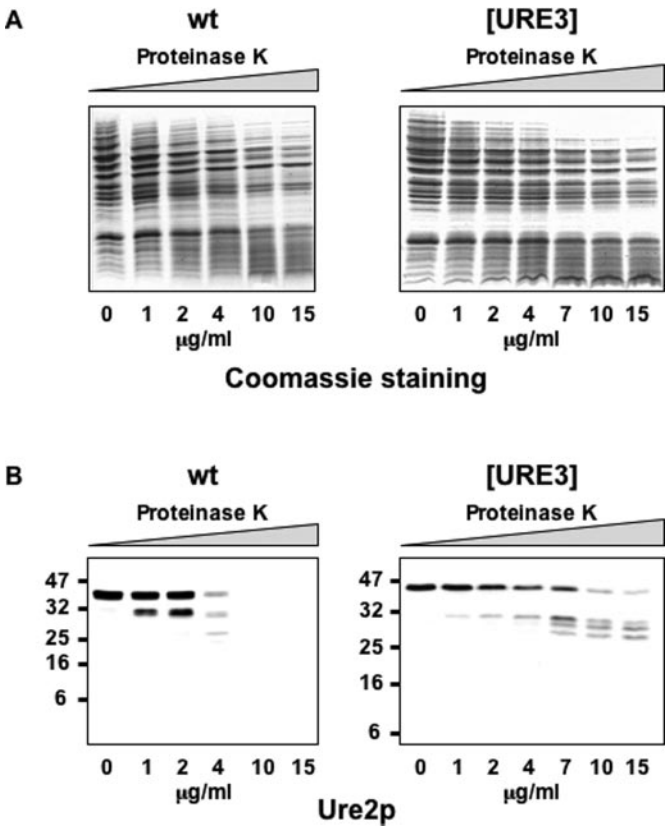

FIG. 3. **Limited proteolysis of Ure2p cellular and prion isoforms.** *A*, total protein extracts were prepared from wild-type and [URE3] strains. They were digested with increasing proteinase K concentrations at 37 °C for 30 min. Samples were analyzed by SDS-PAGE with Coomassie staining. *B*, samples were then analyzed on a Western blot probed with an antibody raised against full-length Ure2p. The numbers on the vertical axis denote the masses of marker proteins (kDa). *wt*, wild-type.

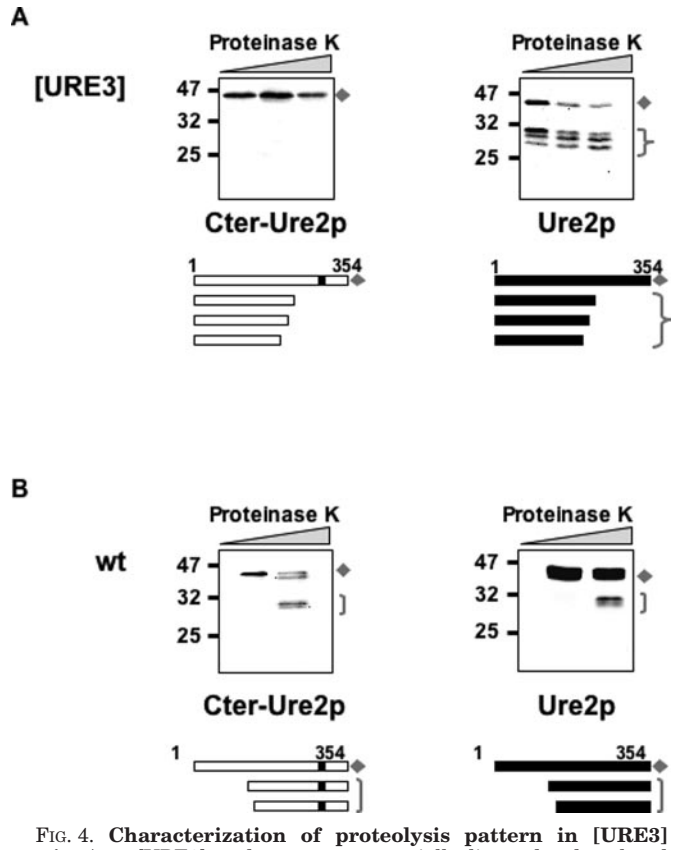

FIG. 4. **Characterization of proteolysis pattern in [URE3] strain.** *A*, an [URE3] crude extract was partially digested and analyzed on Western blot with an antibody raised against a peptide located between amino acids 284 and 298 (*closed box*) in the C-terminal end of Ure2p (*left panel*). From the *left* to the *right*, samples were digested with 7, 10, and 15 µg/ml of proteinase K. The same membrane was reprobed with an antibody raised against full-length Ure2p. The three bands not recognized by the anti-Ure2p$^{284-298}$ antibodies are represented. *B*, a wild-type (*wt*) crude extract was analyzed as in *A*. From the *left* to the *right*, samples were digested with 0 and 1 µg/ml of proteinase K. The bands recognized by the anti-Ure2p$^{284-298}$ antibodies are represented.

was analyzed by Coomassie staining to ensure that proteins were not degraded in the control without proteinase K (Fig. 3*A*). Then, Western blots were performed with antibodies raised against Ure2p. In wild-type extracts, Ure2p was completely digested after a treatment with 10 µg/ml of proteinase K (Fig. 3*B*, *wt* blot). In contrast, full-length Ure2p was still detected with 15 µg/ml of proteinase K in [URE3] extracts (Fig. 3*B*, *[URE3]* blot). Partial degradation of Ure2p from wild-type extracts with 1 µg/ml of proteinase K produced a fuzzy band at 30 kDa, probably corresponding to several fragments arising from different cleavage sites. With higher proteinase K concentration (4 µg/ml), one additional faint band at 25 kDa was observed. When [URE3] crude extracts were analyzed in the same way, a 30-kDa fragment was observed with concentrations of proteinase K ranging from 1 to 4 µg/ml. Two additional fragments of 28 and 26 kDa were detected with increased proteinase K concentration. These three fragments were resistant against up to 50 µg/ml of proteinase K (data not shown). These results clearly indicated that the presence of [URE3] induced a dramatic change in both the resistance and the proteolysis pattern of Ure2p.

To characterize which domains of Ure2p had an increased resistance to proteolysis, an antibody raised against a peptide located in the C-terminal domain of Ure2p, from amino acids 284 to 298, was used to probe the Western blots. In [URE3] extracts, full-length Ure2p was revealed by the "C-terminal" antibody, but none of the three bands in the range of 26–30 kDa was detected (Fig. 4*A*, *Cter-Ure2p*). When the same membrane was incubated with anti-Ure2p antibodies raised against the full-length protein, the full-length Ure2p and the 26–30-kDa fragments were detected (Fig. 4*A*, *Ure2p*). As the fuzzy 30-kDa species generated by controlled proteolysis of wild-type crude extract are recognized by the anti-C-terminal antibodies (Fig. 4*B*), we concluded that the more accessible proteinase K sites of Ure2p in [URE3] cells are different from Ure2p in wild-type.

Limited Proteolysis for Recombinant Soluble Ure2p and Ure2p Amyloid Fibrils—To test whether aggregated Ure2p$^{[URE3]}$was compatible with an amyloid fibril conformation or not, proteolysis patterns of Ure2p extracted from yeast cells were compared with the ones of recombinant soluble Ure2p and Ure2p amyloid fibrils. Ure2p-His$_6$ was expressed and purified from *E. coli*. Amyloid fibrils formation was checked using negative staining electron microscopy (Fig. 5*A*). We first tested the influence of temperature and urea on the solubility of Ure2p. As expected, neither boiling nor adding urea enhanced the level of protein detected by Coomassie staining of SDS-PAGE when the soluble protein was analyzed (data not shown). On the other hand, when the amyloid sample was boiled for 5 min, a massive increase of soluble Ure2p was observed (Fig. 5*B*). Interestingly the presence of urea only slightly changes Ure2p solubility under these conditions. On one hand, urea does not provoke a significant increase in the capacity of Ure2p amyloid fibrils to enter in the polyacrylamide gel (Fig. 5*B*) but on the other hand, under the same conditions, provokes a 5–10-fold increase in the solubility of aggregated Ure2p in [URE3] cells (Fig. 1*A*). This suggests that either the amyloids

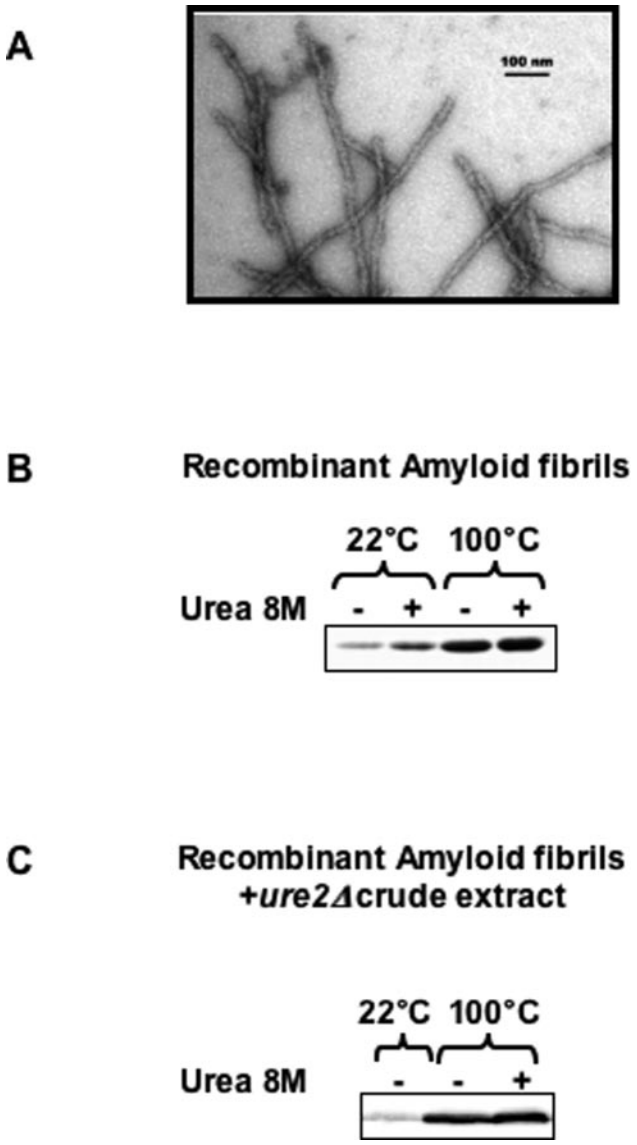

FIG. 5. **Identification of amyloid fibers.** *A*, the formation of amyloid fibrils from soluble Ure2p was checked by negative staining electron microscopy. *B*, the same sample was analyzed by SDS-PAGE with Coomassie staining after boiling or not boiling and adding or not adding urea. *C*, fibrils were incubated 5 min in a *ure2*Δ crude extract before the addition of the sample buffer. Samples were analyzed (after incubation at room temperature or boiling with or without urea) on a Western blot with antibodies against full-length Ure2p.

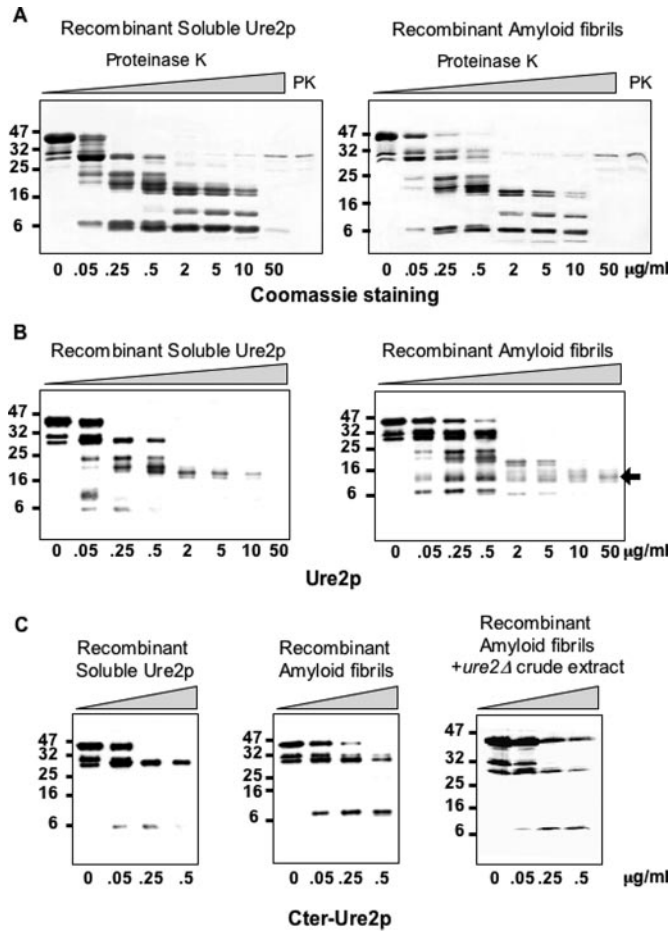

FIG. 6. **Limited proteolysis of recombinant Ure2p.** *A*, recombinant soluble Ure2p and amyloid fibrils were digested with increasing concentrations of proteinase K for 30 min at 37 °C. Samples were analyzed by SDS-PAGE with Coomassie staining. *Lane PK* indicates the control without Ure2p. The *numbers* on the *vertical axis* denote the masses of marker proteins (kDa). *B*, the same samples were analyzed by SDS-PAGE, and Western blots were performed with an antibody raised against full-length Ure2p. The *arrow* indicates a very resistant fragment in amyloid fibrils. *C*, the same samples were analyzed by SDS-PAGE, and Western blots were performed with an antibody raised against a peptide located between amino acids 284 and 298 of Ure2p. Alternatively, amyloid fibrils were incubated with a *ure2*Δ crude extract prior to digestion.

produced *in vitro* are different from *in vivo* aggregates or that amyloids interaction with proteins from yeast crude extract change their sensitivity toward SDS. We therefore tested whether incubation of amyloids with a yeast extract changed their properties. Recombinant amyloid fibrils were incubated in *ure2*Δ crude extract for 5 min prior addition to sample buffer with or without urea. Samples were then incubated for 5 additional min either at room temperature or at 100 °C and analyzed by Western blot. We observed an increase in the Ure2p signal when samples were heated in SDS 2% (Fig. 5*C*). Addition of 8 M urea was not required to efficiently detect this signal (Fig. 5*C*). Therefore, the incubation with a crude extract did not change the solubility properties of the fibrils. We then compared the proteinase K sensitivity of recombinant Ure2p in conditions used to analyze wild-type and [URE3] extracts.

Soluble protein and amyloid fibrils were digested 30 min with proteinase K concentrations ranging from 0 to 50 μg/ml. Digestion patterns were first analyzed by Coomassie staining. Full-length soluble Ure2p is completely degraded with 0.25 μg/ml of proteinase K (Fig. 6*A*, *left*). Digestion with 0.05 μg/ml of proteinase K gave rise to eight fragments with molecular masses around 39, 35, 32, 30, 27, 25, 20, and 6 kDa. The 39-, 35-, 32-, and 27-kDa bands were not detected with higher proteinase K concentrations. The fuzzy 30-kDa band was observed with a proteinase K concentration ranging from 0.05 to 0.5 μg/ml. The 25- and 20-kDa bands were observed at a proteinase K concentration up to 0.5 μg/ml. A 18-kDa fragment is detected after digestion from 0.25 to 10 μg/ml of proteinase K, and another 17-kDa fragment is detected from 0.5 to 10 μg/ml. A 10-kDa band is then observed between 2 and 10 μg/ml of proteinase K. The 6-kDa band is observed at up to 0.5 μg/ml of proteinase K. Finally, a 5-kDa fragment is observed between 0.25 and 10 μg/ml of proteinase K. Ure2p is completely degraded with proteinase K concentrations of 50 μg/ml or more.

The Ure2p amyloid fibril digestion pattern is very similar to the one observed for soluble Ure2p, except for two differences (Fig. 6*A*, *right*). Firstly, the full-length Ure2p is detected with higher proteinase K concentrations than for soluble protein. Indeed the signal is observed up to 0.5 μg/ml of proteinase K.

The second point is an absence of the 39-, 35-, and 27-kDa fragments in amyloid fibrils proteolysis. Other bands are very similar to the ones observed for soluble protein, in terms of size, sensitivity to the same proteinase K concentrations, and relative intensity (Fig. 6*A*, compare soluble Ure2p and amyloid fibrils gels).

These samples were further on analyzed on a Western blot probed with the antibody raised against full-length Ure2p protein. All fragments previously observed on Coomassie staining were detected, except the 10- and 5-kDa fragments (Fig. 6, *A* compare with *B*). An additional fuzzy fragment not stained by Coomassie was detected ~10 kDa in both cases. This species reveals a dramatic change between soluble and amyloid Ure2p. In soluble Ure2p digestion, this fragment could not be detected anymore for a concentration more than 0.05 μg/ml of proteinase K. On the contrary, it exhibits a strong proteolysis resistance, as it is still detected with 50 μg/ml of proteinase K in amyloid fiber digestions. Previous data showed the Ure2p prion-forming domain is highly resistant to proteolysis in amyloid fibrils and that this fragment has a low affinity for Coomassie dye (23). This strongly suggests that this 10-kDa fragment could be the PFD.

Because the 30-kDa fragments are undetectable in [URE3] cells with the anti-C-terminal antibodies, we tested these antibodies on recombinant Ure2p degradation products. Interestingly, these antibodies gave the same proteolysis pattern for soluble (Fig. 6*C*, *left*) or amyloid Ure2p (Fig. 6*C*, *middle*). Only four species (32-, 30-, and 6-kDa and the full-length Ure2p) could be detected. Therefore the digestion pattern of amyloid fibrils differs from [URE3] aggregates pattern. We next tested whether interaction of amyloid fibrils with proteins from a yeast extract could modify the more accessible sites in the fibrils, and as a consequence, change the digestion pattern. Fibrils were incubated in a *ure2*Δ crude extract for 5 min prior to proteolysis. No modification in the digestion pattern was observed (Fig. 6*C*, *right*).

DISCUSSION

In [URE3] strains, Ure2p is converted into a self-propagating inactive form. The conformational changes between the cellular and the prion isoforms of Ure2p remain unknown. Several results related the [URE3] phenotype to an aggregation of Ure2p (24, 28), but the role of these aggregates is still controversial (25–27). Two different models proposed that these aggregates could either be a dead-end product (25–27) or the self-propagating isoform itself (32), called the propagon.

In vitro, Ure2p assembles spontaneously into amyloid-like fibrils (22). The protease digestion of these fibrils reveals a core domain composed of residues 1–70 (23). This domain forms amyloid fibrils in an autocatalytic process. Further on, these aggregates may seed Ure2p aggregation in an amyloid structure (33, 34). The overexpression of this domain also induces an *in vivo* [URE3] appearance (35). But to date, Ure2p amyloids assembled *in vitro* have not been shown to be infectious when introduced into yeast cells. Using green fluorescent protein and Western blot experiments, we recently demonstrated that large aggregates of Ure2p were formed during [URE3] elimination. In [URE3] cells, Ure2p was found in the soluble fraction. Interestingly, the concentration of Ure2p in [URE3] yeast cells was also found to be low.

In this work, we tested whether there was actually less Ure2p in [URE3] cells or whether the prion isoform was difficult to detect in Western blots. We introduced several modifications in our Western blot assay by comparing the buffer composition already used in a previous protocol (28) and observed that urea was necessary to efficiently detect the pelleted Ure2p in [URE3] extracts. Most of Ure2p is therefore aggregated in [URE3] cells. This finding explains the former discrepancies concerning Ure2p aggregation in [URE3] strains, because Schlumpberger and colleagues (28) found Ure2p completely aggregated in [URE3] cells. Moreover, the ratio of aggregated Ure2p depends on the growth conditions. In selective medium, almost all of Ure2p is found aggregated, whereas 20% of the protein remains soluble in yeast cells grown in rich medium. The wild-type phenotype can not be observed when the Ure2p level falls below 15% of the regular level. As a consequence the aggregated protein detected in [URE3] yeast cells can not be functional anymore. This loss of function could be due either to steric constraints or to a conformational change of the globular domain.

The [URE3] aggregates are resistant to boiling in standard SDS buffer. On the contrary, amyloid fibers assembled *in vitro* are efficiently denatured by this treatment and do not require urea to be readily detected. This is also the case if fibers are pre-incubated with a yeast crude extract before SDS treatment. This suggests that Ure2p aggregates formed *in vivo* may be different from *in vitro* generated amyloid fibers. We used limited proteolysis to study these two types of aggregates.

Limited proteolysis is a powerful tool to investigate protein conformation, as accessible regions are preferentially digested. We compared the digestion pattern of the Ure2p protein from wild-type and [URE3] strains to investigate the conformational changes between the cellular and the prion isoforms. As previously observed, the full-length Ure2p protein was more resistant to proteolysis in [URE3] than in wild-type cells (28, 35, 36). The digestion of the Ure2p cellular isoform resulted in a fuzzy 30-kDa band. It is recognized by an antibody raised against a peptide located 8 kDa upstream of the C-terminal end of the protein. As Ure2p is composed of a globular 30-kDa C-terminal domain (37, 38) and a 10-kDa N-terminal PFD that is unstructured (22), we expected that this unstructured domain would be more sensitive to proteinase K. Therefore, the 30-kDa fragment detected in our experiment may be the Ure2p functional domain. This hypothesis is supported by a mass spectrometry analyses of recombinant Ure2p digested by proteinase K, because a 30-kDa fragment was identified as the globular domain of Ure2p (39).

Ure2p [URE3] proteolysis gave a distinct pattern. We observed three bands in the range of 26–30 kDa. Our proteolysis pattern is also found in other yeast strains and also a different prion strain (28), indicating that this property is not restricted to our yeast background but is rather a general feature of [URE3]. None of these three bands was detected with the C-terminal antibody. When using the antibodies raised against the full-length Ure2p, the signal intensity of the 30-kDa fragment reaches the same level as undigested Ure2p. As we clearly detected the full-length protein but none of proteolyzed fragments with the anti-C-terminal antibodies, these fragments do not include the C-terminal end.

The fragments size is consistent with a first cleavage site located 10 kDa upstream from the C-terminal end of Ure2p and two additional sites separated by 2 kDa. These three fragments are very resistant to proteolysis, as they are detected with up to 50 μg/ml of proteinase K. Ure2p aggregation in [URE3] cells therefore confers an increased resistance to proteolysis. It has been clearly demonstrated *in vitro* that the resistant part of Ure2p structured into amyloid fibrils is the first 70 amino acids (23). As the biochemical conditions used during proteinase K treatment and Western blot analysis can influence the results, we then wanted to compare the behavior of the four species, recombinant soluble Ure2p, recombinant amyloid Ure2p, cellular Ure2p, and Ure2p$^{[URE3]}$, under the same experimental conditions.

Only a few differences were observed between the proteolysis patterns of recombinant soluble Ure2p and amyloid fibrils. The first difference is that full-length Ure2p is more protease-resistant when organized in amyloid fibrils. The second is that the 35- and 39-kDa fragments detected in soluble Ure2p digestion are not observed for fibrils. Bousset *et al.* (39) have already shown that these fragments corresponded to a proteolysis at the N terminus of the PFD. This indicated that the cleavage sites in the N terminus were less exposed to the solvent in fibrils. The main difference is the presence of a 10-kDa fragment showing a strongly increased resistance to proteinase K in fibrils. This fragment was not stained by Coomassie dye. Previous work from Baxa *et al.* (23), including mass spectrometry, strongly supported the hypothesis that this fragment may be the PFD. Therefore, the functional domain seems to have the same conformation in fibrils as in soluble protein. This is consistent with the model proposed by Baxa *et al.* (23) concerning Ure2p fibrillation into an amyloid structure. In this model the PFD forms the backbone of the fibrils, surrounded by the functional domain in a largely native conformation (23).

The comparison of soluble and fibrillar Ure2p can not explain the differences found when crude extracts from wild-type or [URE3] cells are compared by the same approach. In [URE3] crude extracts, the first two-thirds of the protein including the PFD and half of the functional domain of Ure2p exhibit a strong resistance to proteinase K. Ure2p fragments that were obtained by [URE3] crude extract proteolysis are only detected after the addition of urea (data not shown). It means that the peptides are still interacting among themselves. On the other hand, Ure2p amyloid fibrils may be analyzed after proteinase K treatment without the addition of urea. This suggests that Ure2p does not form *in vivo* the amyloid structures observed *in vitro*. The difference of behavior between amyloids and [URE3] aggregates could result from the presence of specific partners that would partially cover Ure2p in [URE3] yeast cells. However, the incubation of amyloid fibrils in a yeast crude extract did not change their solubility nor their digestion pattern. This result does not definitively rule out this hypothesis, because such hypothetical partners may interact with Ure2p only during amyloid formation and partially cover Ure2p in [URE3] yeast cells. If this partner exists, it should recognize specifically Ure2p in the aggregated but not the soluble state. This hypothesis is again difficult to combine with the amyloid hypothesis, because *in vitro*, the polymerization of Ure2p in a filament does not lead to apparent structural changes in the globular part of Ure2p.

Alternatively, this pattern may indicate that not only the PFD, but also part of the functional domain could be the core of the aggregates formed *in vivo*. This organization implies that the functional domain of Ure2p undergoes a conformational change between the soluble cellular and the aggregated prion isoform. This hypothesis points the fact that the biochemical nature of the aggregates found in the [URE3] yeast cells remains enigmatic.

Acknowledgments—We thank R. Wickner for the strains 3686 and YHE64. We thank B. Daignan-Fornier and L. Minvielle-Sebastia for the antibodies against Ade13p and Pap1p, respectively. We thank Dr. S. Saupe and Dr. M. Harnasch for many helpful discussions and looking over the English. We thank B. Salin and J. Schaeffer for performing electron microscopy experiments.

REFERENCES

1. Griffith, J. S. (1967) *Nature* **215,** 1043–1044
2. Prusiner, S. B. (1982) *Science* **216,** 136–144
3. Pan, K. M., Baldwin, M., Nguyen, J., Gasset, M., Serban, A., Groth, D., Mehlhorn, I., Huang, Z., Fletterick, R. J., Cohen, F. E., and Prusiner, S. B. (1993) *Proc. Natl. Acad. Sci. U. S. A.* **90,** 10962–10966
4. Legname, G., Baskakov, I. V., Nguyen, H. B., Riesner, D., Cohen, F. E., DeArmond, S. J., and Prusiner, S. B. (2004) *Science* **305,** 673–676
5. Wickner, R. B. (1994) *Science* **264,** 566–569
6. Sondheimer, N., and Lindquist, S. (2000) *Mol. Cell* **5,** 163–172
7. Santoso, A., Chien, P., Osherovich, L. Z., and Weissman, J. S. (2000) *Cell* **100,** 277–288
8. Bach, S., Talarek, N., Andrieu, T., Vierfond, J., Mettey, Y., Galons, H., Dormont, D., Meijer, L., Cullin, C., and Blondel, M. (2003) *Nat. Biotechnol.* **21,** 1075–1081
9. Drillien, R., and Lacroute, F. (1972) *J. Bacteriol.* **109,** 203–208
10. Drillien, R., Aigle, M., and Lacroute, F. (1973) *Biochem. Biophys. Res. Commun.* **53,** 367–372
11. Cox, K. H., Rai, R., Distler, M., Daugherty, J. R., Coffman, J. A., and Cooper, T. G. (2000) *J. Biol. Chem.* **275,** 17611–17618
12. Beck, T., and Hall, M. N. (1999) *Nature* **402,** 689–692
13. Turoscy, V., and Cooper, T. G. (1987) *J. Bacteriol.* **169,** 2598–2600
14. Aigle, M., and Lacroute, F. (1975) *Mol. Gen. Genet.* **136,** 327–335
15. Stansfield, I., Jones, K. M., Kushnirov, V. V., Dagkesamanskaya, A. R., Poznyakovski, A. I., Paushkin, S. V., Nierras, C. R., Cox, B. S., Ter-Avanesyan, M. D., and Tuite, M. F. (1995) *EMBO J.* **14,** 4365–4373
16. Cox, B. S. (1965) *Heredity* **20,** 505–521
17. Paushkin, S. V., Kushnirov, V. V., Smirnov, V. N., and Ter-Avanesyan, M. D. (1996) *EMBO J.* **15,** 3127–3134
18. Patino, M. M., Liu, J. J., Glover, J. R., and Lindquist, S. (1996) *Science* **273,** 622–626
19. Glover, J. R., Kowal, A. S., Schirmer, E. C., Patino, M. M., Liu, J. J., and Lindquist, S. (1997) *Cell* **89,** 811–819
20. King, C. Y., and Diaz-Avalos, R. (2004) *Nature* **428,** 319–323
21. Tanaka, M., Chien, P., Naber, N., Cooke, R., and Weissman, J. S. (2004) *Nature* **428,** 323–328
22. Thual, C., Komar, A. A., Bousset, L., Fernandez-Bellot, E., Cullin, C., and Melki, R. (1999) *J. Biol. Chem.* **274,** 13666–13674
23. Baxa, U., Taylor, K. L., Wall, J. S., Simon, M. N., Cheng, N., Wickner, R. B., and Steven, A. C. (2003) *J. Biol. Chem.* **278,** 43717–43727
24. Edskes, H. K., Gray, V. T., and Wickner, R. B. (1999) *Proc. Natl. Acad. Sci. U. S. A.* **96,** 1498–1503
25. Fernandez-Bellot, E., Guillemet, E., Ness, F., Baudin-Baillieu, A., Ripaud, L., Tuite, M., and Cullin, C. (2002) *EMBO Rep.* **3,** 76–81
26. Fernandez-Bellot, E., Guillemet, E., and Cullin, C. (2000) *EMBO J.* **19,** 3215–3222
27. Ripaud, L., Maillet, L., and Cullin, C. (2003) *EMBO J.* **22,** 5251–5259
28. Schlumpberger, M., Prusiner, S. B., and Herskowitz, I. (2001) *Mol. Cell. Biol.* **21,** 7035–7046
29. Thual, C., Bousset, L., Komar, A. A., Walter, S., Buchner, J., Cullin, C., and Melki, R. (2001) *Biochemistry* **40,** 1764–1773
30. Gietz, R. D., Schiestl, R. H., Willems, A. R., and Woods, R. A. (1995) *Yeast* **11,** 355–360
31. Lingner, J., Kellermann, J., and Keller, W. (1991) *Nature* **354,** 496–498
32. Speransky, V. V., Taylor, K. L., Edskes, H. K., Wickner, R. B., and Steven, A. C. (2001) *J. Cell Biol.* **153,** 1327–1336
33. Schlumpberger, M., Wille, H., Baldwin, M. A., Butler, D. A., Herskowitz, I., and Prusiner, S. B. (2000) *Protein Sci.* **9,** 440–451
34. Taylor, K. L., Cheng, N., Williams, R. W., Steven, A. C., and Wickner, R. B. (1999) *Science* **283,** 1339–1343
35. Masison, D., and Wickner, R. B. (1995) *Science* **270,** 93–95
36. Masison, D. C., Maddelein, M. L., and Wickner, R. B. (1997) *Proc. Natl. Acad. Sci. U. S. A.* **94,** 12503–12508
37. Bousset, L., Belrhali, H., Janin, J., Melki, R., and Morera, S. (2001) *Structure* **9,** 39–46
38. Umland, T. C., Taylor, K. L., Rhee, S., Wickner, R. B., and Davies, D. R. (2001) *Proc. Natl. Acad. Sci. U. S. A.* **98,** 1459–1464
39. Bousset, L., Redeker, V., Decottignies, P., Dubois, S., Le Marechal, P., and Melki, R. (2004) *Biochemistry* **43,** 5022–5032

The [URE3] Yeast Prion Results from Protein Aggregates That Differ from Amyloid Filaments Formed *in Vitro*

Leslie Ripaud, Laurent Maillet, Françoise Immel-Torterotot, Fabien Durand and Christophe Cullin

J. Biol. Chem. 2004, 279:50962-50968.
doi: 10.1074/jbc.M408792200 originally published online September 28, 2004
